

Magnetic properties of a nanocrystalline σ -FeCr alloy

This article has been downloaded from IOPscience. Please scroll down to see the full text article.

2005 J. Phys.: Condens. Matter 17 2985

(<http://iopscience.iop.org/0953-8984/17/19/012>)

View [the table of contents for this issue](#), or go to the [journal homepage](#) for more

Download details:

IP Address: 129.252.86.83

The article was downloaded on 27/05/2010 at 20:43

Please note that [terms and conditions apply](#).

Magnetic properties of a nanocrystalline σ -FeCr alloy

J Cieślak¹, B F O Costa², S M Dubiel^{1,4}, M Reissner³ and W Steiner³

¹ Faculty of Physics and Applied Computer Science, AGH University of Science and Technology, 30-059 Krakow, Poland

² Department of Physics, University of Coimbra, 3000-516 Coimbra, Portugal

³ Institute of Solid State Physics, Vienna University of Technology, 1040 Wien, Austria

E-mail: dubiel@novell.ftj.agh.edu.pl

Received 28 January 2005, in final form 15 March 2005

Published 29 April 2005

Online at stacks.iop.org/JPhysCM/17/2985

Abstract

Magnetic properties of a nanocrystalline σ -Fe_{55.4}Cr_{44.6} alloy were investigated by means of Mössbauer spectroscopy and vibrating sample magnetometry both as a function of temperature ($4 \text{ K} \leq T \leq 300 \text{ K}$) and, for the latter, also as a function of external magnetic field ($B_a \leq 15 \text{ T}$). The methods used enabled us to determine the mean Curie temperature, $\langle T_C \rangle \approx 57 \text{ K}$, and the average magnetic moment per Fe atom, $\langle \mu \rangle = 0.34 \mu_B$, as well as to find that the sample behaves like an ensemble of interacting superparamagnetic particles. Comparison of these results with our recent corresponding investigations on microcrystalline σ -Fe_{100-x}Cr_x alloys with $45 \leq x \leq 50$ shows that the ratio between the average hyperfine field, $\langle B \rangle$, and $\langle \mu \rangle$ for the nanocrystalline sample fits well to that of the microcrystalline ones of similar composition. The non-linear $\langle B \rangle$ - $\langle \mu \rangle$ relationship points to composition-dependent valence hyperfine field contributions.

1. Introduction

σ -FeCr is probably the best known member of the σ -phase family not only because it is the archetype, but mainly due to its mechanical properties, namely high brittleness and hardness, and also technological importance as it precipitates in steels, making them very brittle. In addition, it is one of the two known examples of the binary σ -phases that exhibit magnetic properties. Although the phase was discovered ~ 80 years ago [1], its physical properties, and in particular the magnetic ones, are not precisely known. The magnetism of σ -FeCr is usually termed low temperature weak, because for bulk samples the magnetic order sets in at $T \leq 40 \text{ K}$ and the average magnetic moment per Fe atom, $\langle \mu \rangle$ is smaller than $0.25 \mu_B$ [2, 3]. This means that the magnetism of the σ -FeCr is weaker by a factor of ~ 8 than that of the α -FeCr of similar composition. The magnetism of the σ -FeCr, and, in particular, the low

⁴ Author to whom any correspondence should be addressed.

value of $\langle\mu\rangle$ can be in terms of a localized model interpreted as indicative of a ferrimagnetic order. An alternative, and, probably, more realistic explanation is provided by the itinerant electron model according to which a strong reduction of $\langle\mu\rangle$ could be due to a reduction of the number of spin-up and spin-down electrons in the common band [3]. The Rhodes–Wohlfarth plot [3] and the non-saturating behaviour of the isothermal magnetization curves found in the external field of up to 14 T [4] give strong evidence in favour of the latter model. In view of the lack of a unique description of its physical properties and a wide spread of experimental data, we performed a systematic study of magnetic properties of a series of σ -FeCr alloys in both micro- and nanocrystalline ranges of grain size. In this paper we report on the results obtained for the nanocrystalline σ -Fe_{55.4}Cr_{44.6} sample and compare them with those obtained for microcrystalline ones that will be published in more detail elsewhere [5].

2. Sample preparation and characterization

The nanocrystalline sample was prepared by mechanical alloying using a planetary mill (Fritsch P-7) at a disc rotating speed of 640 rpm, equipped with hardened steel vials and balls (seven pieces) with mixtures of powders of Fe (99.9%, grain size <40 μm) and Cr (99.2%, grain size \sim 100 μm) in argon atmosphere. The weight of the sample powder was 5 g and the powder-to-ball weight ratio was 1:20. The total milling time was 16 h, interrupted for 15 min every hour.

The composition of the sample was determined by microprobe analysis and the result gave Fe_{55.4}Cr_{44.6}. The sample as obtained was found to be 100% in the α -phase as determined by Mössbauer spectroscopy (MS) and x-ray diffraction (XRD) measurements carried out at room temperature.

Transformation of the α -FeCr sample into the σ -phase was successfully performed by isothermal annealing in vacuum at 973 K for 5 h. The verification of the α to σ phase transformation was also done by recording room temperature MS spectra and XRD patterns, which proved that the final phase was 100% sigma.

The XRD technique using Cu K α radiation ($\lambda = 0.154184$ nm) at room temperature was further used to determine the mean crystallite sizes and microstrains, obtained from the widths of the XRD peaks which are shown in figures 1(a) and (b), for the α -FeCr and σ -FeCr samples, respectively, using the Williamson–Hall method [6]. The results gave 10 nm and 0.60% (α -phase) and 27 nm and 0.21% (σ -phase) for mean crystallite sizes and microstrains, respectively. However, as revealed by scanning electron microscopy (SEM) study—see figure 2—the σ -FeCr sample (and also α -FeCr) were in the form of aggregates having the mean size of \sim 30 μm which means that, on average, one agglomerate consists of 10^9 grains. The preparation of the microcrystalline samples is described elsewhere [4].

3. Results and discussion

3.1. Mössbauer measurements

⁵⁷Fe spectra were recorded in transmission geometry using a standard spectrometer and a continuous-flow cryostat with a temperature accuracy better than ± 0.2 K. The gamma rays of 14.4 keV energy were supplied by a ⁵⁷Co/Rh source whose activity enabled measurement of one spectrum of a good statistical quality within a 2 day run. As can be seen in figure 3, even the spectrum recorded at 4.2 K has no well resolved structure, which reflects the weak magnetism of the phase. The asymmetry of the spectrum recorded in the paramagnetic phase (figure 3(b)) can be accounted for with different approaches. Solly and Winqvist, for example, analysed their RT spectrum in terms of four single lines, i.e. they neglected the quadrupole interactions

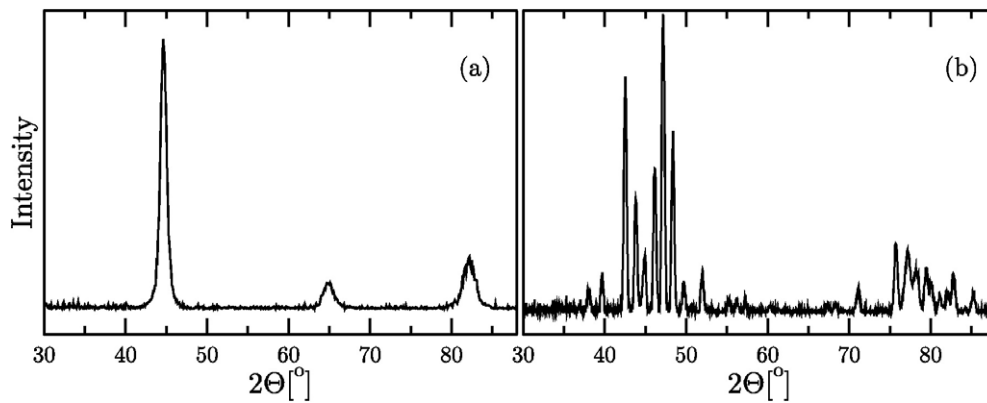


Figure 1. XRD patterns as recorded at RT on nanocrystalline (a) α -FeCr and (b) σ -FeCr samples.

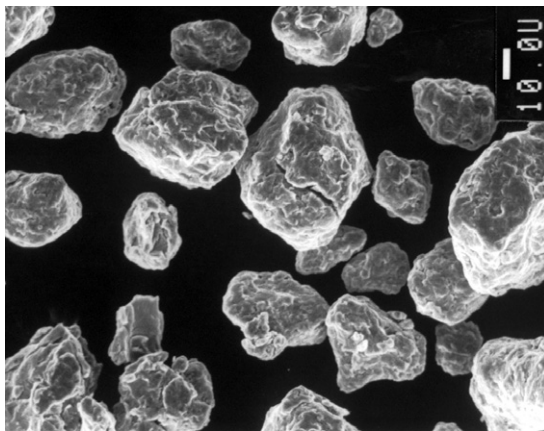


Figure 2. SEM picture of the studied σ -FeCr sample in the form of aggregates. The scale-bar corresponds to 10 μm .

and assumed Fe atoms were present at four sites with different isomer shifts [7]. Gupta *et al* used a three-site model but included the quadrupole interactions in their fitting procedure [8]. Sumimoto and co-workers also fitted their spectra in terms of three subspectra but they neglected the quadrupole splitting [9]. Finally, Cieslak *et al* analysed their paramagnetic spectra of σ -FeCr samples in terms of the distribution of the isomer shift [10]. In other words, due to a low resolution of the spectra (even at low temperature) and actually unknown number of sites occupied by Fe atoms (subspectra), there is no unique way of fitting the spectra. In the present case we wanted to estimate the Curie temperature, which can be obtained from the temperature dependence of the average hf field. For this purpose a model independent method was applied, i.e. the spectra were fitted with a procedure giving the distribution of the hyperfine (hf) field, $P(B)$. It was assumed that the hf field is linearly correlated with the isomer shift, and the average quadrupole splitting is temperature independent. The integration of the $P(B)$ -curves yielded the average hf field, $\langle B \rangle$. From its plot versus T , which can be seen in figure 4, the Curie temperature, $T_C = 55$ K, was determined.

3.2. Magnetization measurements

Measurements of magnetization, M , were carried out with a vibrating sample magnetometer (VSM) in a constant magnetic field, B_a versus temperature, T , as well as at a constant

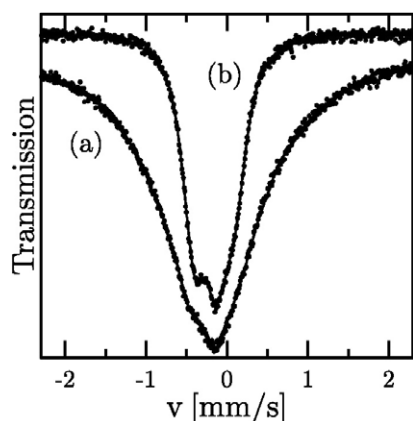


Figure 3. ^{57}Fe Mössbauer spectra recorded at (a) 4.2 K and (b) 65 K on the nanocrystalline $\sigma\text{-Fe}_{55.4}\text{Cr}_{44.6}$ sample. The solid lines are the best fits to the data.

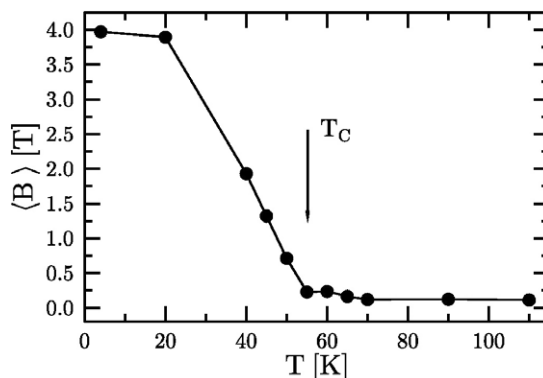


Figure 4. The average hf field, $\langle B \rangle$, as found from the $P(B)$ -curves versus temperature, T . The arrow indicates the Curie point, T_C , and the solid line is to guide the eye.

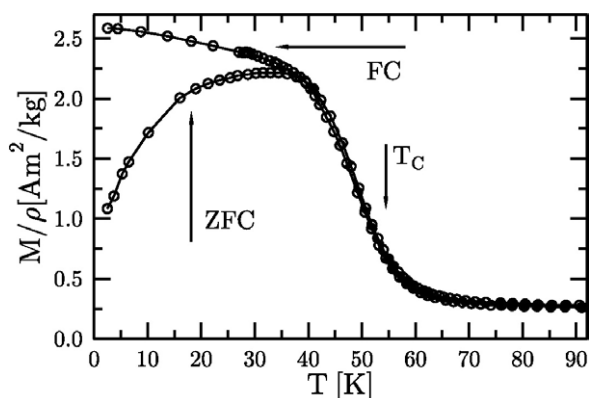


Figure 5. Magnetization, M , versus temperature, T , at $B_a = 0.018$ T. FC stands for the field cooled curve and ZFC for the zero-field cooled one. The solid lines are to guide the eye.

temperature versus B_a . Both measurements enabled determination of T_C . From the $M(T)$ curve taken at $B_a = 0.018$ T, shown in figure 5, $T_C \approx 55$ K was derived, while $T_C \approx 60$ K resulted from the $M(B_a)$ curves analysed in terms of Arrott plots. These two values are close to that found from the average hf field. By extrapolating the linear part of $M(B_a)$ recorded at 4.2 K to $B_a = 0$ T—see figure 6—a value of $\langle \mu \rangle = 0.34 \mu_B$ was found. The negative values of magnetization seen at $B_a = 0$ T follow from the normalization procedure, which was necessary due to the presence of a small fraction of the $\alpha\text{-FeCr}$ phase. All the curves were shifted downwards in such a way that the value of the linear part of the curve measured at 256 K extrapolated to $B_a = 0$ T was equal to zero. The currently found values of $\langle \mu \rangle$ and $\langle T_C \rangle$ are compared in figure 7 with those found recently by us for the microcrystalline samples [4]. As can be seen, the results found for the nanoscale sample seem to be enhanced in comparison with the microcrystalline ones. To verify whether the enhancement is real or merely reflects a non-linear relationship, additional measurements on nanoscale samples containing more chromium are necessary.

The temperature dependence of the magnetization (figure 5) for the nanoscale sample is different for field cooled (FC) and zero-field cooled (ZFC) conditions. This phenomenon is characteristic of superparamagnetic and spin-glass-like behaviour. It can be described with

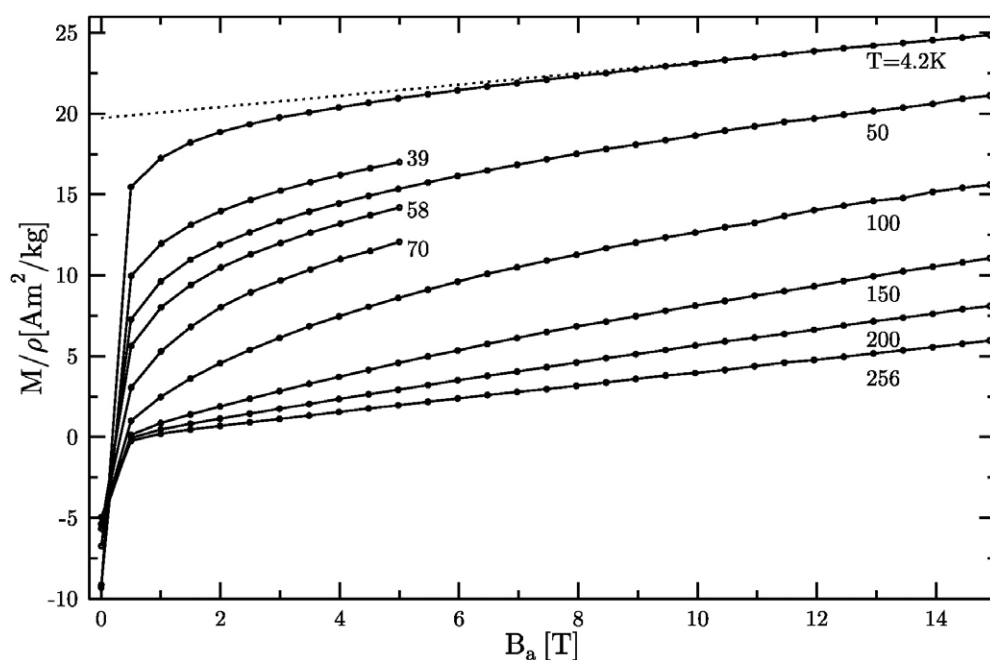


Figure 6. Magnetization measured on the nanocrystalline σ -FeCr sample at constant T shown versus external magnetic field, B_a . The linear part of the curve measured at 4.2 K extrapolated to $B_a = 0$ yielded the magnetic moment.

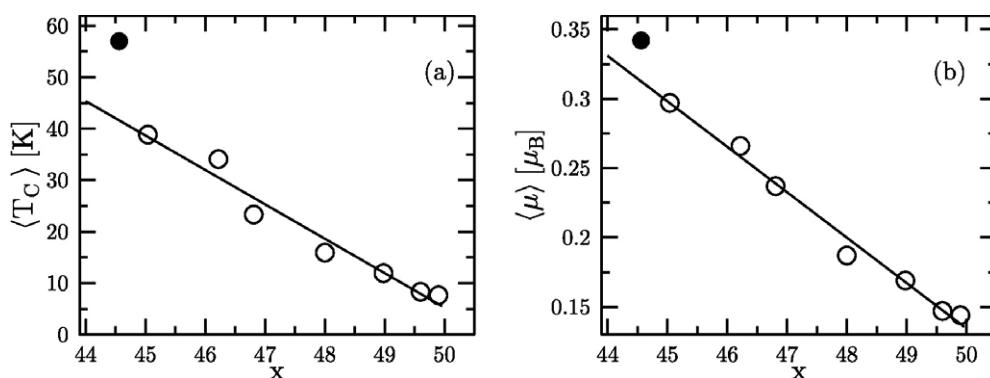


Figure 7. (a) Average Curie temperature, $\langle T_C \rangle$, and (b) average magnetic moment per Fe atom, $\langle \mu \rangle$, versus chromium content, x , as determined by MS and VSM. The solid symbol stands for the nanocrystalline sample and the open symbols for microcrystalline ones [2]. The solid lines represent the best linear fits to the open symbols.

two characteristic temperatures: (1) the temperature T_B , which defines the point at which an irreversibility sets in (T_B corresponds to the blocking temperature of the largest particles [11]), and (2) the maximum temperature, T_M , i.e. the temperature at which the ZFC curve has its maximum (T_M is usually associated with the average blocking temperature). It is of interest to study the influence of B_a both on T_B and on T_M . According to the authors of [12, 13], an increase of T_M with B_a indicates the particles do not interact with each other. Such a behaviour was in fact observed for ferritin [14] as well as for artificially coated particles [15].

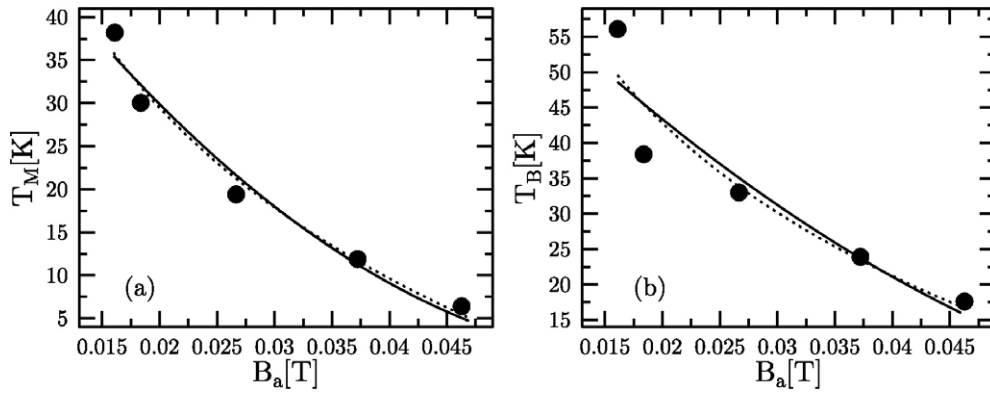


Figure 8. The relation between the external field, B_a , and (a) the maximum temperature, T_M , and (b) the irreversibility temperature, T_B . The best fit to the data in terms of equation (1) is indicated by a solid line and that in terms of equation (2) by a dotted line.

A decrease of T_M with B_a means there is an interaction between particles. This kind of behaviour was also evidenced experimentally [16]. As can be seen in figure 8(a), the latter case also occurs here and this behaviour is consistent with our SEM finding that the investigated sample exists in the form of aggregates with a typical diameter of $\sim 30 \mu\text{m}$, which means that one aggregate consists, on average, of 10^9 interacting nanoparticles. There is not, however, an unique description of the $T_M = f(B_a)$ behaviour. Some authors claim that a quadratic dependence of T_M on B_a gives the right relation between the two quantities [11, 17], while according to others the relation is rather logarithmic [18, 19]. In order to verify which of the two approaches gives a better description of our data, both T_M and T_B were fitted with the following formulae:

$$T_B = \left(\frac{a - B_a}{b} \right)^2 \quad (1)$$

$$T_B = a - b \ln B_a \quad (2)$$

where a and b are free parameters. The best fits of equation (1) to the experimental data are presented in figures 8(a) and (b) as solid lines, and those of equation (2) in the form of dotted lines. As can be seen, both approaches are equally good (which was also reflected in the very similar values of correlation parameters), i.e. based on the present data one is not able to make a distinction between the quadratic and the logarithmic formula.

3.3. Relationship between $\langle B \rangle$ and $\langle \mu \rangle$

It is often assumed for magnetic materials that the hf field is proportional to the magnetic moment. In the case of the average quantities the corresponding formula reads as follows:

$$\langle B \rangle = a \langle \mu \rangle. \quad (3)$$

It should be mentioned that this formula holds quite well for magnetic systems with localized magnetic moments. However, in the case of bcc Fe-based alloys, a two-term formula gives a better agreement with experimental data [20, 21]. In the latter, one term represents a contribution from the polarization of core electrons and another one from the polarization of conduction electrons. Theoretical calculations for pure iron show that only the first term is proportional to the magnetic moment with the proportionality constant a ranging between 9.3

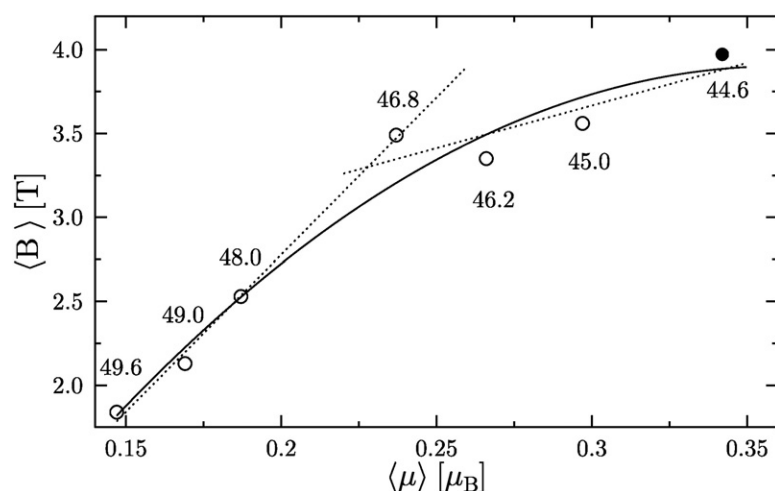


Figure 9. Relation between the average hf field, $\langle B \rangle$, and the average magnetic moment per Fe atom, $\langle \mu \rangle$. The open symbols are for the microcrystalline samples [5], and the full symbol is for the nanocrystalline sample. The figures labelling the symbols represent the concentration of chromium.

and $17.1 \text{ T}/\mu_{\text{B}}$, in dependence on the method of calculation, while the second term is not [22]. Consequently, the departure from formula (3) should be larger for systems whose magnetism is more itinerant than localized. Although there is not a universal value of a even for binary Fe-based systems [23], formula (3) has often been used in practice to determine $\langle \mu \rangle$ from (3) with $a = 15 \text{ T}/\mu_{\text{B}}$ (as estimated from $\langle B \rangle = 33 \text{ T}$ and $\langle \mu \rangle = 2.2 \mu_{\text{B}}$ for α -Fe). Formula (3) was even applied with the same value of a , i.e. $15 \text{ T}/\mu_{\text{B}}$, for a σ -FeCr alloy having a different crystallographic structure to determine $\langle \mu \rangle$ from the knowledge of $\langle B \rangle$ [9]. In order to verify whether this procedure is justified or not for the system of σ -FeCr, we have calculated the a -value for the present case using the measured $\langle B \rangle$ and $\langle \mu \rangle$ -values arriving at $11.5 \text{ T}/\mu_{\text{B}}$. This is close to the value of a found for microcrystalline samples of the σ -FeCr alloys of similar composition, yet significantly less than the value evaluated for the alloys with higher Cr content—see figure 9. In other words, the $\langle B \rangle$ – $\langle \mu \rangle$ relationship for the tetragonal phase of the Fe–Cr system is not linear. The non-linear scaling between $\langle B \rangle$ and $\langle \mu \rangle$ can be understood in terms of the composition dependence of the valence hyperfine field contribution. Such an explanation is very likely in the light of the itinerant character of magnetism in the investigated system [3].

4. Conclusions

Based on the present results, the following conclusions pertinent to the nanocrystalline σ -Fe_{54.4}Cr_{44.6} sample can be drawn.

- The mean Curie temperature $\langle T_{\text{C}} \rangle \approx 57 \text{ K}$, which is significantly more than the value found for a microcrystalline sample of similar composition.
- The average magnetic moment per Fe atom $\langle \mu \rangle_{\text{Fe}} = 0.34 \mu_{\text{B}}$, which is significantly more than the value found for a microcrystalline sample of similar composition.
- The magnetization versus temperature curve, $M(T)$, shows a bifurcation effect which depends on cooling procedure and is characterized with the irreversibility temperature, T_{B} and the maximum temperature, T_{M} .

- (d) Both T_M and T_B decrease with external magnetic field, B_a . The former behaviour indicates the particles interact with each other, and the latter defines the irreversibility line.
- (e) The $T_M(B_a)$ and $T_B(B_a)$ dependences can be equally well described with the quadratic and logarithmic equations.
- (f) Non-linear scaling between $\langle B \rangle$ and $\langle \mu \rangle$ agrees with the itinerant character of the magnetism of the investigated system.

Acknowledgment

Supported by the Austro-Polish Scientific Agreement (project 20/2003).

References

- [1] Bain E C 1923 *Chem. Met. Eng.* **28** 23
- [2] Read D A and Thomas E A 1966 *IEEE Trans. Magn.* **2** 415
- [3] Read D A, Thomas E H and Forsythe J B 1968 *J. Phys. Chem. Solids* **29** 1569
- [4] Cieřlak J, Reissner M, Steiner W and Dubiel S M 2004 *J. Magn. Magn. Mater.* **272–276** 534
- [5] Cieřlak J, Reissner M, Steiner W and Dubiel S M 2005 at press
- [6] Williamson G and Hall W H 1952 *Acta Metall.* **1** 22
- [7] Solly B and Winquist G 1974 *Scand. J. Metall.* **3** 86
- [8] Gupta G, Principi G and Paolucci G M 1990 *Hyperfine Interact.* **54** 805
- [9] Sumimoto Y, Moriya T, Ino H and Fujita F E 1973 *J. Phys. Soc. Japan* **35** 461
- [10] Cieřlak J, Dubiel S M and Sepiol B 1999 *Solid State Commun.* **111** 613
- [11] Mohie-Eldin M E Y, Frankel R B and Gunther L 1994 *J. Magn. Magn. Mater.* **135** 65
- [12] Luo W, Nagel S R, Rosenbaum T F and Rosenzweig R E 1991 *Phys. Rev. Lett.* **67** 2721
- [13] Mann S, Williams J M, Treffy A and Harrison P M 1987 *J. Mol. Biol.* **198** 405
- [14] Dubiel S M, Zablotna-Rypien B, Mackey J B and Williams J M 1999 *Eur. Biophys. J.* **28** 263
- [15] Hanson M, Johansson C and Morup S 1995 *J. Phys.: Condens. Matter* **7** 9263
- [16] Morup S, Bodker F, Hendriksen P V and Linderoth S 1995 *Phys. Rev. B* **52** 287
- [17] Zhang Y D, Budnick J I, Hines W A, Chien C L and Xiao J Q 1998 *Appl. Phys. Lett.* **72** 2053
- [18] Li R W, Xiong H, Sun J R, Li Q A, Wong Z H, Zhang J and Shen B G 2000 *J. Phys.: Condens. Matter* **13** 141
- [19] Roy S, Dubenko I, Edoth D D and Ali N 2004 *J. Appl. Phys.* **96** 1202
- [20] Kuwano H and Ono K 1977 *J. Phys. Soc. Japan* **42** 72
- [21] Elzain M E, Ellis D E and Guenzburger D 1986 *Phys. Rev. B* **34** 1430
- [22] Lindgren B and Sjöström J 1988 *J. Phys. F: Met. Phys.* **18** 1563
- [23] Dubiel S M and Zinn W 1984 *J. Magn. Magn. Mater.* **45** 298